

Piezoelectricity in planar boron nitride via a geometric phase

Matthias Droth,^{1,*} Guido Burkard,¹ and Vitor M. Pereira²

¹*Department of Physics, University of Konstanz, 78457 Konstanz, Germany*

²*Centre for Advanced 2D Materials & Department of Physics,
National University of Singapore, 2 Science Drive 3, Singapore 117542*

Due to their low surface mass density, two-dimensional materials with a strong piezoelectric response are interesting for nanoelectromechanical systems with high force sensitivity. Unlike graphene, the two sublattices in a monolayer of hexagonal boron nitride (hBN) are occupied by different elements, which breaks inversion symmetry and allows for piezoelectricity. This has been confirmed with density functional theory calculations of the piezoelectric constant of hBN. Here, we formulate an entirely analytical derivation of the electronic contribution to the piezoelectric response in this system based on the concepts of strain-induced pseudomagnetic vector potential and the modern theory of polarization that relates the polar moment to the Berry curvature. Our findings agree with the symmetry restrictions expected for the hBN lattice and reproduce well the magnitude of the piezoelectric effect previously obtained *ab-initio*.

PACS numbers: 63.20.kd, 73.22.-f, 77.65.-j, 77.65.Ly

I. INTRODUCTION

Truly two-dimensional materials became a subject of intense research with the experimental isolation of graphene about one decade ago [1–4]. In the wake of the many developments driven initially by research in this graphite monolayer, other two-dimensional crystals such as transition metal dichalcogenides, hexagonal boron nitride (hBN), phosphorene, and others, have gained prominence due to rich and outstanding electronic, magnetic, structural, and optical properties [5–8]. The prospect of stacking individual monolayer materials with different properties holds the promise of a new paradigm in solid state physics as this modular concept of layered van der Waals heterostructures might enable the tailoring of physical properties to levels much beyond the bandgap engineering that is mainstream in semiconductor heterostructures [9, 10]. A key role in such heterostructures would likely fall to hBN. While many two-dimensional building blocks are praised for their superior intrinsic electronic properties, these are detrimentally sensitive to interactions with substrates, other layers, and to contamination [11–13]. With a large bandgap and a lattice mismatch of less than 2% w.r.t. graphene, hBN has the potential to preserve graphene’s celebrated properties within such heterostructures and is currently the insulating substrate of choice for clean, atomically flat deposition or interfacing of two-dimensional crystals [6, 14–18].

Beyond such a passive role, the properties of hBN also allow for an active role. The monolayer of hBN has a honeycomb lattice structure similar to that of graphene, yet one of its two sublattices is occupied by boron (B), and the other by nitrogen (N) atoms, see Fig. 1. This results in a strong ionic bond and a bandgap of ≈ 6 eV

[14, 19–21]. Since inversion symmetry is naturally absent in this crystal, a piezoelectric response is possible [8, 22, 23], i.e., a change in the bulk electric polarization \mathbf{P} when subjected to external stress.

The ability to control bulk polarization mechanically and, conversely, to convert electric fields into mechanical displacements is of enormous interest in the realm of energy harvesting, particularly so at the micro- and nanoscale, where a vision of self-powered miniaturized electronic devices is being strongly pursued in materials science [24–27]. On another front, a strong piezoelectric coupling has been shown to be an important tool in cooling nanoelectromechanical systems (NEMS) to their mechanical quantum ground state [28]. Such applications demand a strong piezoelectric material from the outset and that, in turn, requires a good insulator with a robust interplay between the underlying electronic and mechanic/lattice degrees of freedom. Density functional

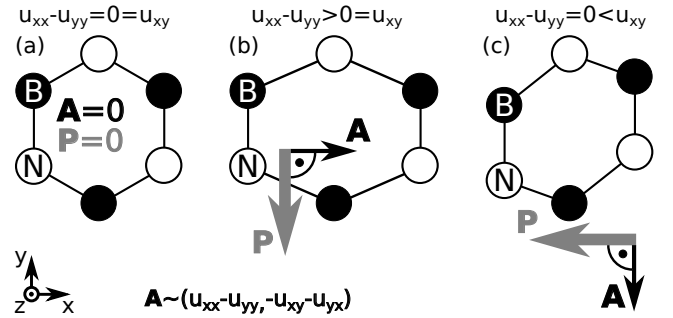


FIG. 1. The lattice of hBN does not possess an inversion center and hence allows for piezoelectricity. (a) Isotropic strain ($u_{xx} = u_{yy}$, $u_{xy} \equiv u_{yx} = 0$) leads to a vanishing pseudomagnetic vector potential \mathbf{A} and does not induce a polarization \mathbf{P} . (b,c) Realizations of the strain tensor u_{ij} that lift the trigonal symmetry and generate a change in the polarization. The induced polarization and the vector potential are always orthogonal, $\mathbf{P} \perp \mathbf{A}$.

* Corresponding author: matthias.droth@uni-konstanz.de

theory (DFT) calculations have established that an hBN monolayer has among the highest specific piezoelectric coefficients (~ 1 pC/N) known [8, 29]. Combined with the lowest surface mass density of all known piezoelectric crystals, this might allow for NEMS with as yet unknown force sensitivity [30]. Moreover, hBN could provide the piezoelectric coupling in a layered graphene/hBN heterostructure and thus allow for the electromechanical manipulation of graphene with an electric field. Its strong piezoelectric characteristics, high mechanical stability, and easy handling make hBN a prime material for such technological applications.

The lattice of (isotropically deformed) hBN does not belong to one of the 10 polar classes and hence, hBN exhibits no spontaneous polarization. However, it does sustain one when subjected to *anisotropic* deformation. In this paper, we use the modern theory of polarization and the geometric phase approach [22, 31, 32] to calculate the electronic contribution to the piezoelectric tensor of hBN in an entirely analytical way. An ionic contribution is not considered, here [33–35]. A DFT calculation in the context of hBN nanotubes established that the dominant electronic contribution ($\approx 80\%$) to the polarization arises from the π valence band, and that it has the same sign as the remaining contribution from the σ valence bands [29, 36, 37]. Therefore, a minimal yet promising ansatz for the analytical description of piezoelectricity in hBN consists in focusing entirely on the π bands. As we demonstrate, the low energy bandstructure of the π bands is already sufficient to derive results in qualitative and good quantitative agreement with DFT calculations.

II. MODEL DETAILS

Due to the underlying honeycomb lattice, low energy electrons in hBN effectively behave as (massive) Dirac fermions. This is similar to the situation in graphene, except for the mass term associated with the different orbital energies at the B and N atoms. The difference in electronegativity between the two species causes electron transfer from B to N within the σ bonds [38] and results in a bond with an ionic character, in contrast to the purely covalent bond of graphene [14, 20]. The broken sublattice symmetry gives rise to the bandgap [39]. Such a model has already been used to describe the chirality-dependent piezoelectric response of hBN nanotubes [22]. In the vicinity of the K points in the hexagonal reciprocal lattice, the effective Hamiltonian is then

$$\mathcal{H}^{(\tau)} = \hbar v_F \boldsymbol{\sigma}^{(\tau)} \cdot (\mathbf{q} - \tau \mathbf{A}), \quad (1)$$

where $\hbar v_F \equiv \frac{3}{2}|t|a$, with $|t|$ as the magnitude of the nearest neighbor tight-binding hopping amplitude and a as the interatomic distance. In the absence of strain, $\mathbf{A} = 0$. In our notation, $\mathbf{q} \equiv (q_x, q_y, \Delta)$, where $q_{x,y}$ are the Cartesian components of the electron's crystal momentum measured relative to the high-symmetry points K ($\tau = +1$) and K' ($\tau = -1$). The vector $\boldsymbol{\sigma}^{(\tau)} \equiv$

$(\tau\sigma_x, \sigma_y, \sigma_z)$ is defined in terms of the three Pauli matrices that address the sublattice degree of freedom (pseudospin) in this problem. Since the real electron spin does not play a role in the following, it is not made explicit in our expressions. The sublattice potential $\hbar v_F \Delta$ arises due to the different on-site energies at the boron ($\Delta > 0$) and nitrogen ($-\Delta$) atoms, and gives rise to a bandgap of $2\hbar v_F \Delta$ in hBN. When $\mathbf{A} = 0$, the energy dispersion associated with Eq. (1) is the hyperbola

$$E_{c,v}(\mathbf{q}) = \pm \hbar v_F (q_x^2 + q_y^2 + \Delta^2)^{1/2} \quad (2)$$

centered at each K point. The vector \mathbf{A} encodes the electron-lattice coupling for anisotropic strains and provides the essential mechanism through which the system can sustain a strain-induced polarization. It is well known that the effect of such lattice deformations can be accounted for via the pseudomagnetic vector potential \mathbf{A} in the Hamiltonian $\mathcal{H}^{(\tau)}$. The form of Eq. (1) aptly reflects the minimal-type substitution $\mathbf{q} \mapsto \tilde{\mathbf{q}} \equiv \mathbf{q} - \tau \mathbf{A}$, where the pseudomagnetic vector potential is given by [3, 40, 41]

$$\begin{pmatrix} A_x \\ A_y \\ A_z \end{pmatrix} \equiv \frac{3t\beta\kappa}{4\hbar v_F} \begin{pmatrix} u_{xx} - u_{yy} \\ -u_{xy} - u_{yx} \\ 0 \end{pmatrix}. \quad (3)$$

This definition is given in terms of the strain tensor $u_{ij} \equiv (\partial_i u_j + \partial_j u_i)/2$, where $\mathbf{u}(\mathbf{r})$ is the local displacement field, in general a function of position, although here we shall focus on strictly uniform and planar strain configurations. The parameter $\beta \equiv \frac{a}{t} \frac{\partial t}{\partial a} < 0$ describes the variation of the hopping amplitude $t < 0$ w.r.t. bond length in linear order and $\kappa \sim 1$ [40]. In Sec. V, we discuss the complete prefactor/coupling strength in detail. The electron-phonon coupling encoded in \mathbf{A} has the qualitative effect of displacing the center of the Fermi circles from $\tau \mathbf{K}$ to $\tau(\mathbf{K} + \mathbf{A})$ [42]. This affects the Berry curvature in the parameter space (q_x, q_y, λ) , where $\lambda \in [0, \Delta]$ parametrizes the sublattice potential.

In a microscopic description of strain-induced electrical polarization, one formally and conventionally identifies two additive contributions [33, 43, 44]. The first one, so called ionic contribution, arises from the breakdown of the Cauchy-Born rule and the need to explicitly consider relative ionic displacements within the crystal's unit cell that are not accounted for by the macroscopic strain field u_{ij} . This ionic contribution can be characterized analytically if an accurate empirical force constant model to describe the lattice degrees of freedom is known [45]. In the case of hBN, such calculations were performed by Michel and Verberck [34, 35]. The second, electronic contribution arises from the induced electronic density and is the specific focus of this paper, computed within the quantum phase approach [31, 44]. From an *ab-initio* standpoint, a common strategy to identify these two contributions consists in (i) computing the *electronic* polarization as a function of strain while keeping the ions clamped and (ii) performing the same computation with

fully relaxed ions, which yields the *total* (electronic and ionic) polarization. Note that the ionic and electronic contributions have opposite sign for hBN [8, 33, 35, 38].

To determine the electronic contribution to the piezoelectric constant of an hBN monolayer, we conceive a gedankenexperiment in which the gap parameter in Eq. (1) varies adiabatically from $\lambda = 0$ (graphene) to $\lambda = \Delta$ (hBN). Such adiabatic change is accompanied by the development of a bulk polarization — induced dipole moment per unit area — whose magnitude is obtained from [22, 32, 46]

$$P_i = 2e \sum_{\tau} \int_0^{\Delta} d\lambda \int_{\text{BZ}/2} \frac{d^2 q}{(2\pi)^2} \Omega_{q_i, \lambda}^{(\tau)}. \quad (4)$$

Here, P_i is the i -th Cartesian component of the induced polarization vector, $e = |e|$ is the unit charge, and the factor of 2 accounts for the spin degeneracy. The integral over half the Brillouin zone (BZ) around each valley combined with the summation over τ recovers the full BZ integral required. The Berry curvature is given by

$$\Omega_{q_i, \lambda}^{(\tau)} \equiv i \left\langle \frac{\partial u_{\tau}}{\partial q_i} \left| \frac{\partial u_{\tau}}{\partial \lambda} \right\rangle - i \left\langle \frac{\partial u_{\tau}}{\partial \lambda} \left| \frac{\partial u_{\tau}}{\partial q_i} \right\rangle, \quad (5)$$

where $|u_{\tau}\rangle$ is a valence eigenstate of Eq. (1) with $\Delta \mapsto \lambda$.

III. STRAIN-INDUCED POLARIZATION

From Eq. (5), one straightforwardly resolves the Berry curvatures

$$\Omega_{q_x, \lambda}^{(\tau)} = -\tau \frac{\tilde{q}_y}{2\epsilon^3}, \quad \Omega_{q_y, \lambda}^{(\tau)} = \tau \frac{\tilde{q}_x}{2\epsilon^3}, \quad (6)$$

where $\epsilon \equiv |E_{c,v}(\tilde{q}_x, \tilde{q}_y, \lambda)|$. To be specific, we consider now the calculation of P_x according to Eq. (4). Integration over the adiabatic parameter leads to

$$\int_0^{\Delta} d\lambda \frac{\tau \tilde{q}_y}{\epsilon^3} = \frac{\tau \Delta \tilde{q}_y}{(\tilde{q}_x^2 + \tilde{q}_y^2) \sqrt{\tilde{q}_x^2 + \tilde{q}_y^2 + \Delta^2}}. \quad (7)$$

This is followed by the momentum integration over a square $[-w, +w]^2$ centered at each of the two high symmetry points K and K' of the undistorted BZ. To conserve the total number of states, the area of each square is exactly half of the first BZ zone, i.e. $w = 3^{3/4}K/4 = 3^{-3/4}\pi/a$. After restoring the prefactor, this BZ integration leads to an entirely analytical expression for P_x (and likewise for P_y). For piezoelectricity, the linear response of \mathbf{P} w.r.t. strain is relevant. As Eq. (3) shows that \mathbf{A} is linear in strain, it is appropriate to focus on the leading order of the induced polarization in the pseudomagnetic vector potential:

$$\mathbf{P} = \frac{2e}{\pi^2} \tan^{-1} \left[\frac{\Delta}{\sqrt{2w^2 + \Delta^2}} \right] \mathbf{A} \times \hat{\mathbf{z}} + \mathcal{O}(A^3). \quad (8)$$

This is the main result of our analytic calculation. On one hand, it manifests a new and useful qualitative result: the

pseudomagnetic vector potential and the induced polarization are orthogonal, $\mathbf{P} \perp \mathbf{A}$, irrespective of the state of strain. On the other hand, the exact and simple analytical expression in Eq. (8) allows us to extract definite quantitative predictions regarding the magnitude of the piezoelectric coefficient in hBN.

IV. PIEZOELECTRIC TENSORS AND SYMMETRY

The components of the direct and converse piezoelectric tensors are, respectively, given by

$$d_{ijk} \equiv \frac{\partial P_i}{\partial \sigma_{jk}}, \quad e_{ijk} \equiv \frac{\partial P_i}{\partial u_{jk}}, \quad (9)$$

where σ_{jk} is the stress tensor. The crystal of hBN belongs to the point group $\bar{6}m2$ (D_{3h}) which, for the lattice orientation introduced in Fig. 1 containing a mirror plane perpendicular to the x -axis, imposes the symmetry constraints

$$\begin{aligned} d_{211} &= d_{112} = d_{121} = -d_{222}, \\ e_{211} &= e_{112} = e_{121} = -e_{222}, \end{aligned} \quad (10)$$

while all other components vanish identically [47]. The piezoelectric response is thus characterized by only one number, and we call d_{222} and e_{222} the direct and converse piezoelectric constants, respectively. The direct and converse effects are related through the elastic tensor, $e_{ijk} = d_{imn} C_{jkmn}$, which, since we have only one independent component in each, reduces to the simple relation $e_{222} = d_{222}(C_{2222} - C_{2211})$. To confirm consistency of our model with symmetry constraints, note that Eq. (8) implies $(\partial P_x / \partial A_y) = -(\partial P_y / \partial A_x)$. Together with Eq. (3), this leads to, e.g.,

$$e_{222} = \frac{\partial P_y}{\partial A_x} \frac{\partial A_x}{\partial u_{yy}} = -\frac{\partial P_x}{\partial A_y} \frac{\partial A_y}{\partial u_{xx}} = -e_{112}. \quad (11)$$

Analogously, we can verify that all the relations in Eq. (10) are indeed satisfied by the model. The piezoelectric constant is explicitly given by

$$e_{222} = \frac{e|\beta|\kappa}{\pi^2 a} \tan^{-1} \left[\frac{\Delta}{\sqrt{2w^2 + \Delta^2}} \right]. \quad (12)$$

V. MAGNITUDE OF THE PIEZOELECTRIC CONSTANT

The electromechanical coupling strength $\frac{3}{4}t\beta\kappa$ in Eq. (3) arises from a low energy approximation of a tight-binding Hamiltonian that describes electronic hopping among the p_z orbitals of neighboring atoms in the honeycomb lattice of hBN [40]. Under strain, the interatomic distances are changed and the hopping amplitude $t < 0$ is modified accordingly. This couples the electronic system to the lattice degrees of freedom to an extent that is controlled by the parameter $\beta \equiv \frac{a}{t} \frac{\partial t}{\partial a} < 0$ which reflects the

sensitivity of the hopping amplitude to changes in the bond length. Since, as in graphene, the π band comes about due to electron hopping between the p_z -orbitals of nearest-neighboring atoms, t corresponds to the Slater-Koster parameter $V_{pp\pi}$, and it is natural to expect an exponential decay of t with increasing interatomic distance [48, 49]. In analogy with a parametrization that is fairly accurate in graphene [42, 50], we consider

$$t(a) = t_0 e^{\beta(a-a_0)/a_0}, \quad (13)$$

where $t_0 \equiv t(a_0)$ denotes the hopping amplitude at the equilibrium bond length a_0 . We can estimate β from existing data for the Slater-Koster parameters $V_{pp\pi}$ in hBN with first-, second-, and third-nearest neighbors that are fit to accurately reproduce the bandstructure obtained from DFT calculations [8, 15, 20, 51]. Both the first- and the third-nearest neighbor hopping occur between B and N atoms. With $t_0 = t^{(1)} = t(1.44 \text{ \AA}) = -2.16 \text{ eV}$ and $t^{(3)} = t(2.88 \text{ \AA}) = -0.08 \text{ eV}$ for the first and third neighbor hopping amplitudes, respectively, we find $\beta = -3.3$, which is a value very similar to that for graphene [50]. This similarity is not surprising as the atomic orbitals involved are the same in the two systems, and the relaxed interatomic distance is nearly the same, too. For consistency of $t^{(1)}$ and $t^{(3)}$, we have used the values from Ref. [51] in our estimate for β . However, literature values for the nearest neighbor hopping amplitude cumulate rather around $t_0 = -2.3 \text{ eV}$ and we thus infer $t\beta = 7.6 \text{ eV}$ [14, 15, 52]. The dimensionless parameter κ depends on microscopic details of the lattice dynamics. In lowest order of a valence-force-field model [40, 45], it is given by $\kappa = 1/\sqrt{2}$. This results in an electromechanical coupling strength of $\frac{3}{4}t\beta\kappa = 4.0 \text{ eV}$ in Eq. (3). Putting this together with all the other relevant parameters listed in Table I, we evaluate Eq. (12) and finally estimate the contribution of the π electrons to the total piezoelectric constants to be

$$\begin{aligned} e_{222} &\simeq 0.63 \text{ e/nm} = 1.0 \times 10^{-10} \text{ C/m}, \\ d_{222} &\simeq 2.8 \text{ e}/\mu\text{N} = 0.44 \text{ pC/N}. \end{aligned} \quad (14)$$

Duerloo *et al.* obtained the values $e_{222} \simeq 1.38 \times 10^{-10} \text{ C/m}$ in a fully relaxed-ion DFT calculation and $e_{222} \simeq 3.71 \times 10^{-10} \text{ C/m}$ under clamped-ion conditions (note that our coordinate convention is different from the one used by these authors) [8]. As described earlier, the latter corresponds to the electronic contribution and is the one appropriate for direct comparison with the figures quoted in Eq. (14) since our model accounts only for the electronic part. We further recall that our calculation hinges entirely on the electronic effects associated with π -band electrons, justified by the fact that, according to first principles calculations, these account for 80 % of the electronic piezoelectric response [29]. This factor of 0.8^{-1} can be incorporated in our results allowing us to refine the numbers in Eq. (14) to $e_{222} \simeq 1.3 \times 10^{-10} \text{ C/m}$ and $d_{222} \simeq 0.55 \text{ pC/N}$ as the prediction for the electronic contribution to the piezoelectric constants. Given the

Quantity	Value	Quantity	Value
β	-3.3	κ	0.71
w	0.96 \AA^{-1}	a	1.44 \AA
Δ	0.60 \AA^{-1}	$C_{2222} - C_{2211}$	229 N m^{-1}

TABLE I. The parameter β is discussed around Eq. (13) and κ follows from a lowest order valence-force-field model [40, 45]. The value for a stems from Refs. [15, 17] and is also used for $w = 3^{-3/4}\pi/a$. With $t = -2.3 \text{ eV}$ [14, 15, 52] and $\hbar v_F = 3|t|a/2$, Δ corresponds to a bandgap of $2\hbar v_F\Delta = 6.0 \text{ eV}$ [15, 19–21]. For $C_{2222} - C_{2211}$, we use the elastic constants $C_{11} = 291 \text{ N/m}$ and $C_{12} = 62 \text{ N/m}$, as reported in Ref. [8] (Voigt notation; different lattice orientation).

uncertainty inherent to our estimate of the electromechanical coupling strength $\frac{3}{4}t\beta\kappa$ above, we consider this result to be in good quantitative agreement with the first principles value of $3.71 \times 10^{-10} \text{ C/m}$. Beyond the scope of the current work, it would be interesting to obtain *ab-initio* a more precise value of the logarithmic derivative of the hopping, β , so the quantitative accuracy of our model can be fully assessed.

We reiterate the impressive magnitude of the piezoelectric response in hBN already pointed out by Duerloo *et al.* as well as Michel and Verberck [35]. For comparison, the piezoelectric tensor components of quartz vary in the range $d \sim 0.7 - 2.3 \text{ pC/N}$ [53]. The numbers in Eq. (14) show that a single, atomically thin layer of hBN is essentially as good a piezoelectric as a crystal of quartz.

VI. CONCLUSION

We have obtained exact analytical results for the induced polarization and piezoelectric constant of monolayer hBN within the quantum geometric phase approach. In our minimal model, which is proven to satisfy the symmetry constraints expected for the point group $\bar{6}m2$ (D_{3h}), the interaction between deformations and the electronic degrees of freedom is captured in the effective two-band Hamiltonian via a pseudomagnetic vector potential. Ionic degrees of freedom are not considered. Using existing literature estimates for the relevant bandstructure parameters and elastic constants in this system, we find that the converse and direct piezoelectric constants for this model are as high as $e_{222} = 1.3 \times 10^{-10} \text{ C/m}$ and $d_{222} = 0.55 \text{ pC/N}$, respectively. The strain-induced polarization \mathbf{P} is exactly perpendicular to the pseudomagnetic vector potential \mathbf{A} .

We also provide an estimate for the so far unknown coupling strength of the strain-induced pseudomagnetic vector potential in hBN, namely, $\frac{3}{4}t\beta\kappa = 4.0 \text{ eV}$. That the magnitude of the piezoelectric coefficient obtained here agrees well with the value extracted from independent DFT calculations attests to the validity and pertinence of the minimal model, especially since it provides a simple analytical result for its dependence on the basic ma-

terial parameters. Another advantage of our calculation is that, through Eqs. (1) and (8), one can interpret the piezoelectric effect in this material as a consequence of the displacement of the Dirac point under strain from its default position at K in the BZ: a measurement of the electric polarization is thus an indirect measure of how much and along which direction the Dirac point drifts from K under strain.

Our findings for atomically flat hBN might be ultimately put to test in hopefully upcoming experiments which, to our knowledge, have not been reported yet. We thus provide an analytical and concise description of piezoelectricity in hBN that is of relevance for the understanding of nanoscale devices containing hBN as a piezoelectric component, including — but not limited to —

heterostructured NEMS based on two-dimensional materials.

VII. ACKNOWLEDGEMENTS

MD and GB thank the European Science Foundation and the Deutsche Forschungsgemeinschaft (DFG) for support within the EuroGRAPHENE project CONGRAN and the DFG for funding within SFB 767 and FOR 912. VMP was supported by the National Research Foundation (Singapore) under its Medium Sized Centre Programme and CRP grant “Novel 2D materials with tailored properties: Beyond graphene” (Grant No. NRF-CRP6-2010-05).

-
- [1] K. S. Novoselov, A. K. Geim, S. V. Morozov, D. Jiang, Y. Zhang, S. V. Dubonos, I. V. Grigorieva, and A. A. Firsov, *Science* **306**, 666 (2004).
 - [2] G. Eda, G. Fanchini, and M. Chhowalla, *Nat. Nanotechnol.* **3**, 270 (2008).
 - [3] A. H. Castro Neto, F. Guinea, N. M. R. Peres, K. S. Novoselov, and A. K. Geim, *Rev. Mod. Phys.* **81**, 109 (2009).
 - [4] Y.-M. Lin, C. Dimitrakopoulos, K. A. Jenkins, D. B. Farmer, H.-Y. Chiu, A. Grill, and Ph. Avouris, *Science* **327**, 662 (2010).
 - [5] K. S. Novoselov, D. Jiang, F. Schedin, T. J. Booth, V. V. Khotkevich, S. V. Morozov, and A. K. Geim, *Proc. Natl. Acad. Sci. U.S.A.* **102**, 10451 (2005).
 - [6] C. R. Dean, A. F. Young, I. Meric, C. Lee, L. Wang, S. Sorgenfrei, K. Watanabe, T. Taniguchi, P. Kim, K. L. Shepard, and J. Hone, *Nat. Nanotechnol.* **5**, 722 (2010).
 - [7] B. Radisavljevic, A. Radenovic, J. Brivio, V. Giacometti, and A. Kis, *Nat. Nanotechnol.* **6**, 147 (2011).
 - [8] Karel-Alexander N. Duerloo, Mitchell T. Ong, and Evan J. Reed, *J. Phys. Chem. Lett.* **3**, 2871 (2012).
 - [9] K. S. Novoselov, V. I. Fal’ko, L. Colombo, P. R. Gellert, M. G. Schwab, and K. Kim, *Nature (London)* **490**, 192 (2012).
 - [10] A. K. Geim and I. V. Grigorieva, *Nature (London)* **499**, 419 (2013).
 - [11] Kentaro Nomura and Allan H. MacDonald, *Phys. Rev. Lett.* **96**, 256602 (2006).
 - [12] Jian-Hao Chen, Chuang Jang, Shudong Xiao, Masa Ishigami, and Michael S. Fuhrer, *Nat. Nanotechnol.* **3**, 206 (2008).
 - [13] J.-H. Chen, C. Jang, S. Adam, M. S. Fuhrer, E. D. Williams, and M. Ishigami, *Nat. Phys.* **4**, 377 (2008).
 - [14] John Robertson, *Phys. Rev. B* **29**, 2131 (1984).
 - [15] J. Sławińska, I. Zasada, and Z. Klusek, *Phys. Rev. B* **81**, 155433 (2010).
 - [16] L. Britnell, R. V. Gorbachev, R. Jalil, B. D. Belle, F. Schedin, A. Mishchenko, T. Georgiou, M. I. Katsnelson, L. Eaves, S. V. Morozov, N. M. R. Peres, J. Leist, A. K. Geim, K. S. Novoselov, and L. A. Ponomarenko, *Science* **335**, 947 (2012).
 - [17] W. Paszkowicz, J. B. Pelka, M. Knapp, T. Szyszko, and S. Podsiadlo, *Appl. Phys. A* **75**, 431 (2002).
 - [18] M. T. Allen, O. Shtanko, I. C. Fulga, A. R. Akhmerov, K. Watanabe, T. Taniguchi, P. Jarillo-Herrero, L. S. Levitov, and A. Yacoby, *Nat. Phys.* **12**, 128 (2016).
 - [19] Kenji Watanabe, Takashi Taniguchi, and Hisao Kanda, *Nat. Mater.* **3**, 404 (2004).
 - [20] M. Topsakal, E. Aktürk, and S. Ciraci, *Phys. Rev. B* **79**, 115442 (2009).
 - [21] Somnath Bhowmick, Abhishek K. Singh, and Boris I. Yakobsen, *J. Phys. Chem. C* **115**, 9889 (2011).
 - [22] E. J. Mele and Petr Král, *Phys. Rev. Lett.* **88**, 056803 (2002).
 - [23] Xuedong Bai, Dmitri Golberg, Yoshio Bando, Chunyi Zhi, Chengchun Tang, Masanori Mitome, and Kenji Kurashima, *Nano Lett.* **7**, 632 (2007).
 - [24] Zhong Lin Wang and Jinhui Song, *Science* **312**, 242 (2006).
 - [25] Wenzhuo Wu, Lei Wang, Yilei Li, Fan Zhang, Long Lin, Simiao Niu, Daniel Chenet, Xian Zhang, Yufeng Hao, Tony F. Heinz, James Hone, and Zhong Lin Wang, *Nature (London)* **514**, 470 (2014).
 - [26] B. C. Regan, S. Aloni, K. Jensen, R. O. Ritchie, and A. Zettl, *ACS Nano Lett.* **5**, 1730 (2005).
 - [27] Hanyu Zhu, Yuan Wang, Jun Xiao, Ming Liu, Shaomin Xiong, Zi Jing Wong, Ziliang Ye, Yu Ye, Xiaobo Yin, and Xiang Zhang, *Nat. Nanotechnol.* **10**, 151 (2015).
 - [28] A. D. O’Connell, M. Hofheinz, M. Ansmann, Radosław C. Białczak, M. Lenander, Erik Lucero, M. Neeley, D. Sank, H. Wang, M. Weides, J. Wenner, John M. Martinis, and A. N. Cleland, *Nature (London)* **464**, 697 (2010).
 - [29] Na Sai and E. J. Mele, *Phys. Rev. B* **68**, 241405(R) (2003).
 - [30] J. Scott Bunch, Arend M. van der Zande, Scott S. Verbridge, Ian W. Frank, David M. Tanenbaum, Jeevak M. Parpia, Harold G. Craighead, and Paul L. McEuen, *Science* **315**, 490 (2007).
 - [31] David Vanderbilt, *Phys. Rev. B* **41**, 7892 (1990).
 - [32] Di Xiao, *Rev. Mod. Phys.* **82**, 1959 (2010).
 - [33] Stefano Baroni, Stefano de Gironcoli, and Andrea Dal Corso, *Rev. Mod. Phys.* **73**, 515 (2001).

- [34] K. H. Michel and B. Verberck, Phys. Rev. B **80**, 224301 (2009).
- [35] K. H. Michel and B. Verberck, Phys. Rev. B **83**, 115328 (2011).
- [36] Ivan Naumov, Alexander M. Bratkovsky, and V. Ranjan, Phys. Rev. Lett. **102**, 217601 (2009).
- [37] S. M. Nakhmanson, A. Calzolari, V. Meunier, J. Bernholc, and M. Buongiorno Nardelli, Phys. Rev. B **67**, 235406 (2003).
- [38] The transfer of negative charge from B to N within the σ bond is overcompensated by the charge transfer within the π bond which gives the boron atom an effective negative charge in equilibrium [45].
- [39] B. Hunt, J. D. Sanchez-Yamagishi, A. F. Young, M. Yankowitz, B. J. LeRoy, K. Watanabe, T. Taniguchi, P. Moon, M. Koshino, P. Jarillo-Herrero, and R. C. Ashoori, Science **340**, 1427 (2013).
- [40] Hidekatsu Suzuura and Tsuneya Ando, Phys. Rev. B **65**, 235412 (2002).
- [41] C. L. Kane and E. J. Mele, Phys. Rev. Lett. **78**, 1932 (1997).
- [42] Vitor M. Pereira, A. H. Castro Neto, and N. M. R. Peres, Phys. Rev. B **80**, 045401 (2009).
- [43] Stefano de Gironcoli, Stefano Baroni, and Raffaele Resta, Phys. Rev. Lett. **62**, 2853 (1989).
- [44] Raffaele Resta, Rev. Mod. Phys. **66**, 899 (1994).
- [45] Walter A. Harrison, *Electronic Structure and the Properties of Solids* (W. H. Freeman and Company, San Francisco, 1980).
- [46] R. D. King-Smith and David Vanderbilt, Phys. Rev. B **47**, 1651 (1993).
- [47] J. F. Nye, *Physical Properties of Crystals* (Oxford University Press, New York, 1957).
- [48] J. C. Slater and G. F. Koster, Phys. Rev. **94**, 1498 (1954).
- [49] D. A. Papaconstantopoulos and M. J. Mehl, J. Phys. Condens. Matter **15**, R413 (2003).
- [50] R. M. Ribeiro, Vitor M. Pereira, N. M. R. Peres, P. R. Briddon, and A. H. Castro Neto, New J. Phys. **11**, 115002 (2009).
- [51] Paul Giraud, *Study of the Electronic Structure of Hexagonal Boron Nitride on Metal Substrates* (Master thesis, Université des Sciences et Technologies Lille 1, 2012).
- [52] R. M. Ribeiro and N. M. R. Peres, Phys. Rev. B **83**, 235312 (2011).
- [53] R. Bechmann, Phys. Rev. **110**, 1060 (1958).